

ASR testing versus field experience in Austria

Helga Zeithhofer ⁽¹⁾, Birgit Achleitner ⁽²⁾, Gerald Maier ⁽³⁾, Clémence Bos ⁽⁴⁾, Martin Peyerl ⁽⁵⁾, Stefan Krispel ⁽⁶⁾

(1) Smart Minerals GmbH, Vienna, Austria, email Zeithhofer@smartminerals.at

(2) Smart Minerals GmbH, Vienna, Austria, email Achleitner@smartminerals.at

(3) Smart Minerals GmbH, Vienna, Austria, email Maier@smartminerals.at

(4) Smart Minerals GmbH, Vienna, Austria, email Bos@smartminerals.at

(5) Smart Minerals GmbH, Vienna, Austria, email Peyerl@smartminerals.at

(6) Smart Minerals GmbH, Vienna, Austria, email Krispel@smartminerals.at

Abstract

In the last decades the problem of damaging ASR (alkali-silicate-reaction) in Austrian road constructions was gaining increasing attention. Therefore, test methods to quantify the reactivity of aggregates were implemented. Based on the RILEM AAR-2 and RILEM AAR-3 recommended testing methods, an accelerated mortar-bar test, and a long term test for concrete prisms, were introduced with minor amendments at national level (ÖNORM B 3100). Regarding road constructions, it was recognised that field experience and test results concerning the reactivity of aggregates, do not necessarily fit together.

The present work gives a first insight of a project that attempts to close the gap between laboratory results and field experience by mineralogical, structural, chemical and standard ASR testing methods (RILEM AAR-2, RILEM AAR-3) on samples from 6 different quarries. Mortar-bar tests and long term tests of aggregates used in road constructions were performed to determine the expansion potential. Parallel, thin sections of the aggregates were prepared to analyse the mineralogical composition, as well as the texture and the quartz fabrics. For the estimation of the field-side situation, drill cores from different locations with reactive aggregates were taken. Micro and macro structures were investigated and compared with the laboratory results with respect to the life time of the construction. Furthermore, the gradation of alkalinity from the surface to the bottom concrete layer, which equilibrated through years in use, was analysed by different analysis techniques e.g. LA-ICP-MS and μ -XRF to quantify the long-term-equilibrium of alkalis between input from de-icing salts and leaching through precipitation. The results from laboratory and field-side created new insights of the damaging behaviour of ASR and the mineralogical properties of reactive aggregates.

Keywords: ASR in road constructions; alkalis in concrete; concrete microscopy; evaluation of ASR testing

1. INTRODUCTION

Alkali-silica reaction (ASR) is a deterioration process in concrete leading to substantial damages of structures worldwide [1, 2]. During the last decades the prevention of damaging ASR in concrete have become more and more efficient. One reason for this trend is a better understanding of occurring processes in concrete, especially of the chemical and physical nature of the reactions between pore-water and the aggregates (ASR). Hence, damages in concrete can be better assigned to their real cause. Scientists from all over the world consider the reaction of alkaline pore solution in concrete with amorphous (or cryptocrystalline) quartz from the aggregates as the underlying model of the formation of damaging ASR [3-9]. The main parameters for the reaction are the reactivity of the aggregates, the amount of soluble alkalis within the concrete and environmental conditions (moisture, temperature) [1,2,3,9].

Further parameters like admixtures in concrete and the main constituents of cement influence the formation of a damaging ASR. For example, long-time experience in Austria shows that the use of cement with a relatively high amount (up to 35 %) of blastfurnace slag (CEM II/A(B)), is very much responsible for a mitigation and overall very marginal occurrence of damaging ASR in the national road network [15]. Also fly ash, trass (natural pozzolana) and metakaolinite (calcined clays) can be

used as concrete admixture to reduce the ASR potential. Other main constituents of cements or additions like fly ash increase the ASR resistance by alkaline binding.

Based on the current state of research [10, 11] the significant factor for ASR-products to occur in concrete is the chemical and mineralogical composition of the raw materials. For the prevention of concrete damaging ASR, alternative standards in practical implementation are needed.

Concrete damages forced by ASR weren't of great interest in Austria for a long time. It was widely accepted that the national aggregates have a very low alkali-reactive potential which does not lead to damages in concrete. A reason for the small number of ASR-damages might be the combination of national aggregates with slag containing cements, which generally slow the ASR reaction down. However in the last decades the problem of damaging ASR in Austrian road constructions was gaining increasing relevance [15]. One reason for this evolution is a better differentiation of damaging processes by suitable methods like concrete microscopy. The Austrian guidelines for testing the ASR potential are currently methods to classify the aggregates, based on the RILEM AAR-2 and RILEM AAR-3 method (described in chapter 2).

In this study we want to present first intermediate results from the project "AKR performance" (funded by the Austrian research funding agency FFG). One of the main targets is to compare results from laboratory testing with real experience from road constructions. Six different aggregates were analysed chemically and mineralogically with regard to their quartz fabric.

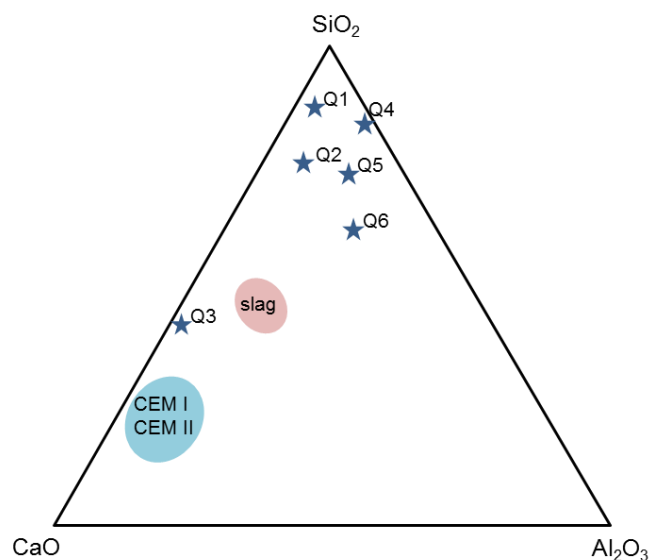


Figure 1.1: Chemical composition of the investigated aggregates in the ternary CaO-SiO₂-Al₂O₃ plot

The structural fabric of 10 to 15 years old concrete in pavements, constructed with the investigated aggregates (Q1 – Q6), was evaluated microscopically and compared with the classification of standard testing methods. Furthermore the concentration of alkalis from road drill cores was quantified, using laser ablation ICP-MS (LA-ICP-MS) on drill core cross sections and atomic absorption spectroscopy (AAS) on bore dust. The results were compared with the concentration of alkalis in testing specimens of ÖNORM B 3100, after one year storage in 4 percent NaOH. Aim is to compare the content of alkalis between field and laboratory conditions to evaluate possible enrichment factors in both conditions. Furthermore μ -XRF mapping on dry cut drill core cross sections was performed and compared with the results from LA-ICP-MS and AAS.

2. METHODS

2.1 Petrographic analyses

Qualitative analyses on aggregates and concrete structures were performed on thin sections embedded in fluorescent epoxy resin on a NIKON Eclipse Ci-Pol microscope. The quartz fabric is classified with regard to microstructure according to Passchier and Trouw [12] and divided in following

groups: 1) intracrystalline deformation (deformation lamellae, undulöse extinction), 2) recovery (subgrains, deformation bands), 3) dynamic recrystallization (Bulging (BLG), Subgrain rotation (SGR), grain boundary migration (GBM), 4) statically quartz (magmatic quartz, grain boundary area reduction (GBAR)), 5) sedimentary quartz (cherts, chalcedon, pressure solution).

2.2 ASR testing

Due to the intense exposure of road constructions in Austria by de-icing salt, freeze and thaw cycles and infiltration of moisture preventive guidelines (ÖNORM B 3100 [16], ÖNORM B 3327-1 [17]) to assess the alkali-silica reactivity of aggregates were introduced. An overview of the testing method is given in Table 2.1. The Austrian guideline consists of a rapid mortar test which is based on the RILEM AAR-2.2 [18] (mortar bar test) and a long-term prism test.

According to the guideline ÖNORM B 3100 – Evaluation of the ASR in concrete, two exposure classes were discriminated:

Exposure class 1: (low to medium)

Exposure class 2: (high, road pavement)

Aggregates of exposure class 2 are uncritical if long-time experience of minimum 20 years exists and no ASR damages have been documented. Aggregates without long-time experience have to be tested by rapid mortar prism test (15 days) defined in the guideline ÖNORM 3100. If the evaluation is negative a long-term concrete prism test (12 month) can be performed.

Table 2.1: Overview of the ASR guideline ÖNORM B 3100 in Austria

Parameter	rapid testing	long-term testing
size testing prism	4x4x16 cm	10x10x40(±4) cm
used aggregates [mm]	0.125 – (all aggregate sizes: commonly up to 32 mm)	pretended sieve curve (aggregates commonly 22 mm)
duration [weeks]	2	52
temperature storage [°C]	80±2	38±2
amount of alkalis	1-molar NaOH solution	1-molar NaOH
threshold value of expansion	1.0 ‰	EW: 0.5 ‰ MW: 0.7 ‰

2.2.1 Rapid testing

The rapid ASR test method is performed on mortar prisms (4x4x16 cm) which are produced with standard cement CEM I 42.5 R. After 24 hours the prisms are demoulded and slowly heated in water to a temperature of 80 °C. After 24 hours under water the prisms are stored in pre-heated 1-molar NaOH-solution of 80 °C for 13 days. The classification of the aggregates is based on the total expansion of the mortar prisms during their storage in NaOH-solution (2nd – 14th day after initial measure) without consideration of the thermal expansion of the prisms.

2.2.2 Long-term testing

For long-term testing concrete prisms (10x10x40(±4) cm) are produced using CEM I 42.5 R. After 24 hours the prisms are demoulded and kept at 20 °C and ≥90 % humidity for another 6 days. Afterwards the prisms were stored in pre-heated 1-molar NaOH solution of 38 °C for 51 weeks. The classification of the aggregates is based on the total expansion of the concrete prisms during storage in NaOH-solution without consideration of the thermal expansion of the prisms.

2.3 Analytical methods for alkalis

2.3.1 Determination of the concentration of alkalis on bore dust

Am minimum amount of 5 g of bore-dust was gained through drilling from laboratory and real-life samples. Sample digestion was conducted according to ÖNORM EN 13657 [19] in aqua regia using a laboratory microwave (ethos.start, MLS GmbH, Germany). Analysis was performed by AAS (iCE 3000 Atomic Absorption Spectrometer, ThermoFisher Scientific, Germany).

2.3.2 Determination of the concentration of alkalis by laser ablation ICP-MS

For LA-ICP-MS measurements, drill cores with a diameter of 5 cm were prepared. Maximum sample size was 5.0x2.5x10.0 cm due to the size limits of the ablation chamber. All cuts were executed without cooling water to prevent analyte loss. Before analysis, loose dust was removed from the sample surface using clean and dry pressurized air.

For the combined determination of alkalis (Na and K) and chloride, mortar prisms with various amounts of potassium chloride, sodium chloride and sodium nitrate were produced for external calibration. To achieve a low background signal during measurements a cement with low alkali equivalent was selected. Before mixing, the alkali salts were dissolved in water. Prism fabrication was accomplished with a laboratory mixer (Toni MIX 1551, Toni Technik, Germany). Alkali contents were reviewed according to ÖNORM EN 196-2 [20]. Analytical concentrations in the mortar prisms are shown in Table 2.2.

Table 2.2: Analyte content in calibration samples.

	BLK	1	2	3	4	5
	m% (in relation to cement content)					
Na	0.41	0.56	0.72	0.93	1.21	1.97
K	0.98	1.23	1.36	1.67	1.80	2.60
Cl	0.11	0.26	0.42	0.64	0.92	1.56

All measurements were performed using a quadrupole ICP-MS device (iCAP Q, ThermoFisher Scientific, Germany) coupled to an NWR213 laser ablation unit (ESI, USA). Instrumental parameters were chosen according to Bonta et al [21]. Analysis of elemental distribution was performed using consecutive linescans over the sample surface. For quantification, every sample line was divided into 18 segments with equal length. Data points in each segment were averaged and a blank value representing the signal without material ablation was subtracted. Measured intensities were normalized using the calcium signal (^{42}Ca) as internal standard. Segment selection to exclude aggregates from examination was done using the ^{27}Al and ^{42}Ca median signal intensity. Concluding, the remaining segment values were averaged to obtain representative mean values for each investigated line.

2.3.3 Analysis of alkalis by Micro-XRF

A drill core from a ten year old road-surface and a laboratory sample after one year storage in a 4 percent NaOH solution were chosen for μ -XRF analysis. To prevent analyte leaching the samples were cut without cooling water. All measurements were performed using the M4 TORNADO^{PLUS} from Bruker nano, equipped with a super light element micro-XRF spectrometer and a specifically optimized Rh X-ray tube. A step size of 75 μm (scan resolution 2413 x 600 pixels), dwell time of 15 ms/pixel and excitation of 50 kV and 600 μA for the Rh-tube were chosen for element mapping.

3. RESULTS

3.1 Petrographic description of the aggregates

An overview of the chemical and mineralogical composition of the different aggregates is given in Table 3.1. XRF and XRD measurements were performed on the fraction 4/8. Petrographic analyses of hard rocks (Q4, Q5 and Q6) were investigated on field samples and the gravel samples (Q1, Q2 and Q3) were conducted on the grain size 4 – 8 cm.

XRD analyses were performed using a Panalytical XPert Pro MPD diffractometer, Cu LFF tube, 45 kV, 40 mA and a X'Celerator detector (acquisition time 25 s, step size 0,017° from 3° to 70° 2 Theta). The quantification of the phases was carried out with Rietveld refinement, using the software X'Pert High Score Plus from Pananalytical.

The occurring quartz fabric is classified in terms of formation and deformation processes, as described in chapter 2.1. Figure 3.1 illustrates the most frequent occurring quartz fabric of the aggregates in the respective quarry.

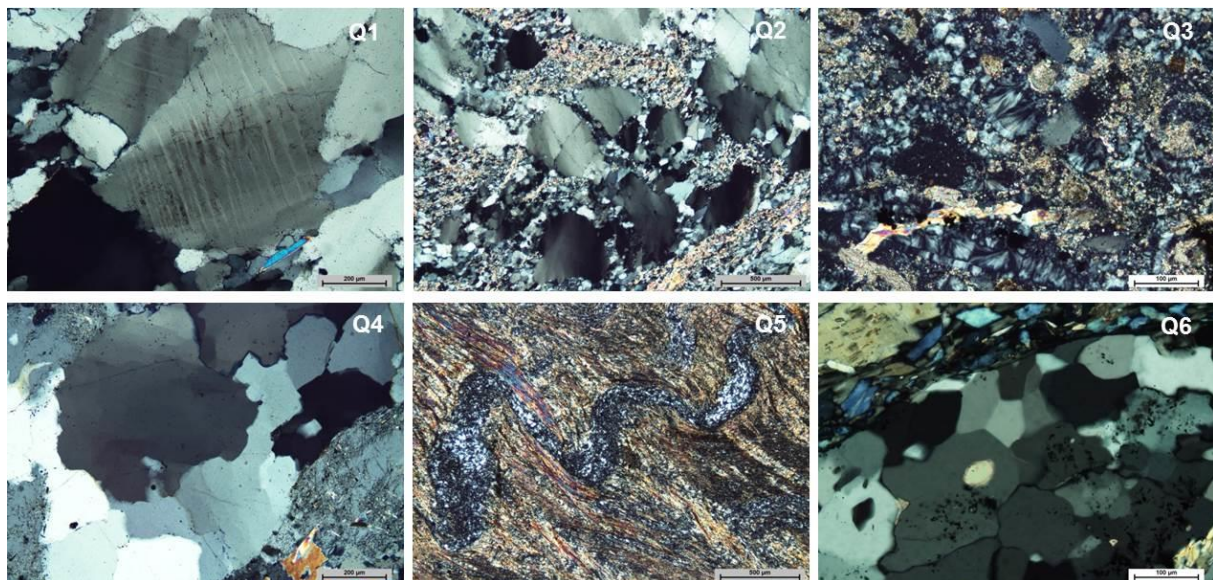


Figure 3.1: Q1: intracrystalline deformation, deformation lamellae; Q2: dynamic recrystallisation, subgrain rotation (SGR); Q3: sedimentary quartz, chalcedony; Q4: dynamic recrystallisation, grain boundary migration (GBM); Q5: pressure solution, folded vein; Q6: grain boundary area reduction, triple junctions

Table 3.1: Overview of the chemical and mineralogical composition for the aggregates

	Quarry 1 siliceous gravel	Quarry 2 mixed gravel	Quarry 3 carbonaceous gravel	Quarry 4 Para-gneiss	Quarry 5 metamorphic diorite	Quarry 6 metamorphic diabase
Chemistry (XRF, m%)						
LOI	8.3	9.6	32.9	0.4	7.1	3.0
SiO ₂	75.0	63.7	24.4	74.4	53.1	47.8
CaO	9.2	13.4	33.2	0.7	7.0	11.1
Al ₂ O ₃	2.8	6.7	1.2	13.2	12.6	17.3
MgO	1.9	1.2	6.6	0.4	3.3	7.3
Fe ₂ O ₃	1.4	2.9	1.0	2.0	8.7	8.4
Na ₂ O	0.6	1.4	0.2	2.6	3.6	2.9
Na _{equ}	0.96	2.15	0.30	6.38	4.69	2.96
Mineralogy (XRD, m%)						
quartz	67	51	23	36	18	1
calcite	11	20	46	0	10	3
dolomite	7	0	27	0	0	0
plagioclase	7	18	0	16	31	40
potassium feldspar	4	0	0	33	12	0
amphibole	2	6	0	0	0	20
pyroxen	0	0	0	0	2	0
chlorite	1	3	2	1	15	18
mica	1	2	2	7	2	0
zoisite/epidot	0	0	0	0	3	17
aluminosilicates/garnet	0	0	0	7	0	0
iron phases (ilmenite, haematite, magnetite)	0.01	0.01	0.01	0,01	6	1
Quarz fabric						
1) intracrystalline deformation (deformation lamellae, undulöse extinction)	X	X	X	X	X	---
2) Recovery (subgrains, deformation bands)	X	X	---	---	---	---
3) Dynamic recrystallization (Bulging (BLG), Subgrain rotation (SGR), grain boundary migration (GBM))	X	X	---	X	X	X
4) statically quartz (magmatic quartz, grain boundary area reduction (GBAR))	---	---	---	---	---	X
5) Sedimentary quartz (cherts, chalcedon, pressure solution)	X	---	X	---	pressure solution in veins	---

3.2 Expansion by standard testing

Rapid tests on aggregates of the six investigated quarries were performed. The maximum grain size of the aggregates was 32 mm. The aggregates were crushed and sieved; the grading curve according ÖNORM B 3100 was complied. The expansion development is illustrated in Figure 3.2.

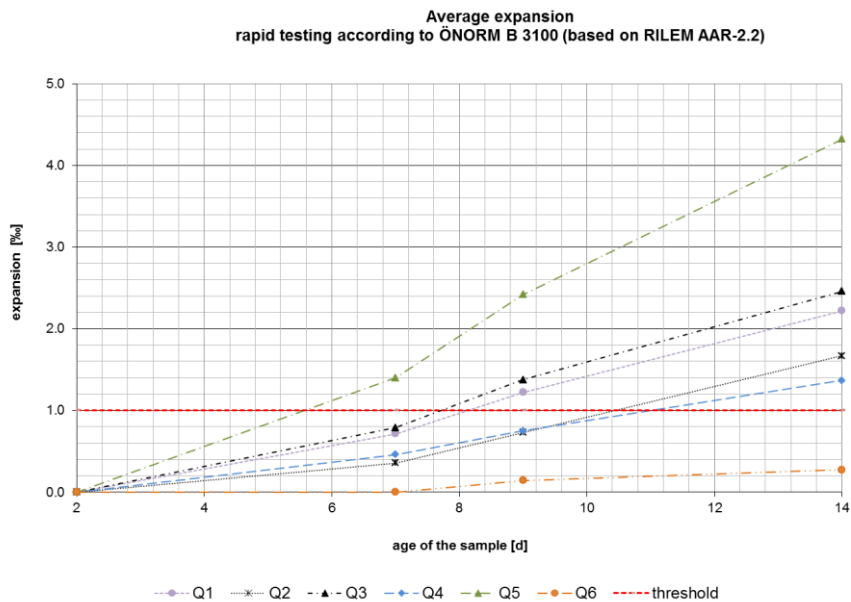


Figure 3.2: Expansion after rapid testing according to ÖNORM B 3100 (standard deviation $\leq 0,03$ per measurement point); threshold expansion: 1‰

All of the tested samples, except Q6 are reactive aggregates according to the Austrian Standard ÖNORM B 3100. The final expansions of the aggregates do not consistently fit with the total amount of Na_{equ} or quartz, or with the ration of Na_{equ} to available Quartz in the mineral composition. The sedimentary samples from fluvoglacial quarries (Q1, Q2, Q3) and the paragneis sample (Q4) show a direct correlation of the final expansion and the Na_{equ} (Figure 3.3, left). This relation exists also between expansion and the ratio of quartz to Na_{equ} . The aggregates with basaltic composition (Q5, Q6) do not fit in this concept.

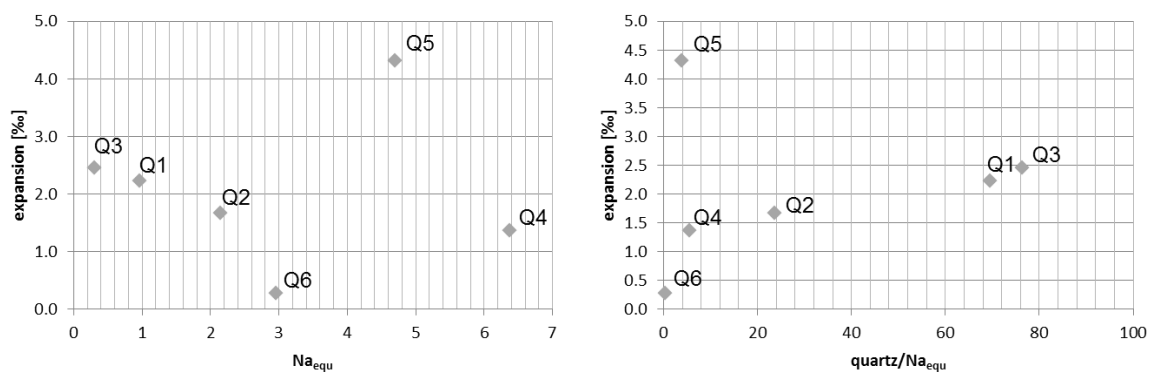


Figure 3.3: left: relationship between expansion (acc. ÖNORM B 3100, rapid testing) and Na_{equ} ; right: relationship between expansion and the product of Na_{equ} with the ratio of quartz to SiO_2

3.3 Comparison field versus laboratory samples

3.3.1 Microstructures

Drill cores of ten year old road constructions, containing aggregates of the above described quarries have been taken to investigate micro- and macrostructures of the concrete. On the basis of the ASR test results, which suggest a reactive behaviour for most of the aggregates (Q1-Q5), a high amount of ASR-products and cracking was expected to occur within the samples.

But surprisingly macrostructures and microstructures did not confirm damaging properties of the aggregates. Only a very little amount of ASR products could be observed inside air voids and cracking (plastic cracks $<10\ \mu\text{m}$) occurred very rarely within all the field samples. The microstructure of a long-term tested laboratory sample (Q1) was investigated for comparison. The amount of occurring ASR-products and also the micro-cracking was much higher than in the field samples, see Figure 3.4.

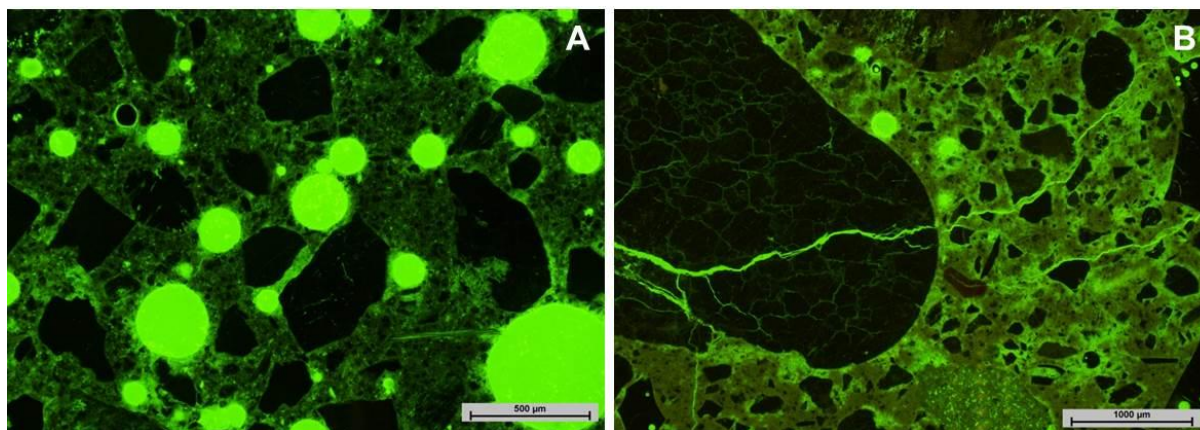


Figure 3.4: Microstructures of concrete, photographs are performed using fluorescent light; A: concrete sample from a ten year old road construction with entrained air; no micro-cracking occurs; air voids are free of ASR products; B: laboratory sample without entrained air; brittle microcracking can be observed all over the sample

A reason for this different behaviour is the different concrete recipe of the samples from the laboratory and the field samples. Especially the cement type, content and the water to cement ratio, together with the aggregates directly influence the geochemical initial situation and consequently the thermodynamics of the whole system. Proceeding from this stand, a performance concept for the testing of specific concrete compositions seems appropriate.

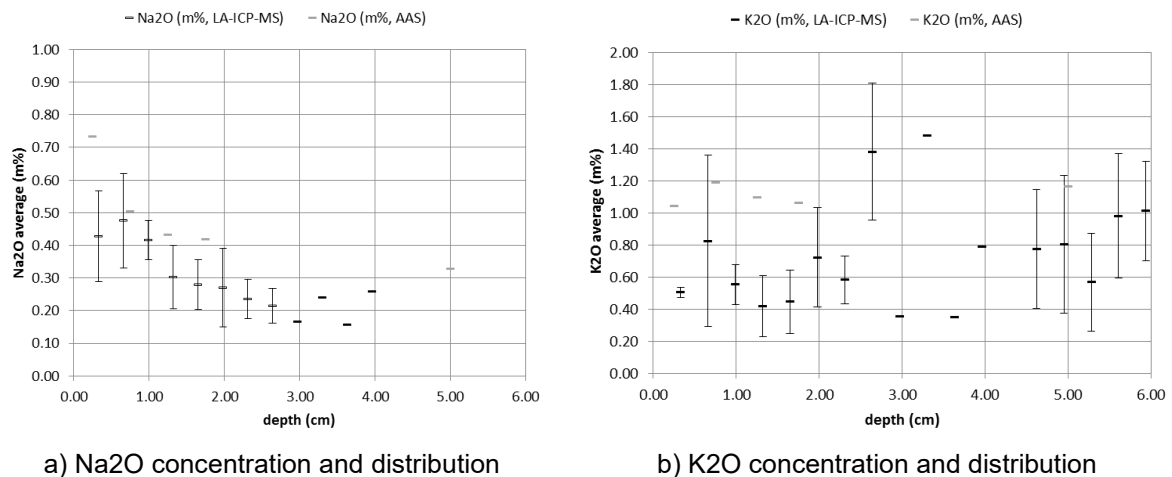
In addition the environment in the field favours reaction much less as the laboratory conditions. In the lab-test the concrete is permanently exposed to an abundance of alkalis (from the surrounding solution) and to a very high temperature. In contrast the field-concrete is only exposed to alkalis during winter and low temperatures and is most of the time in a dry state where ASR is also effectively prevented.

Another important point is the amount and behaviour of added external alkalis on the concrete surface, and the mobility within the concrete structure. The comparison of the total amount of alkalis of ten year old field samples from road constructions and from laboratory samples after one year storage in 4 percent NaOH is presented in chapter 3.3.2.

3.3.2 Alkali enrichment

For evaluation of real-time exposure a field sample in the shape of a drill core from road construction was analysed using different measurement techniques. Examination of alkali concentration and distribution was conducted using LA-ICP-MS for direct analysis and AAS for digested bore dust samples. Comparable contents for Na_2O and K_2O were gained with both techniques as shown in Figure 3.5, whereas LA-ICP-MS provided more detailed information concerning element distribution as higher spatial resolution was possible. For the field sample, Na_2O accumulation was observed in the outer regions (0 – 2 cm). The concentration of Na_2O by LA-ICP-MS on the surface of the road construction is determined in the range of 0.3 – 0.55 m% and settles to ~ 0.25 m% below 2 cm of the concrete surface. Measured concentrations by AAS are slightly higher and range from 0.73 m% Na_2O

on the surface to 0.3 at a level of 5 cm below the surface. Both techniques indicate a similar enrichment of Na₂O on the surface of factor 2.2 by AAS and 2.1 by LA-ICP-MS. For Potassium uniform allocation was noted, concentrations range around 0.7 for LA-ICP-MS and 1.1 for AAS measurements.



a) Na₂O concentration and distribution b) K₂O concentration and distribution

Figure 3.5: concentration and distribution of alkalis of a drill core from road construction; left: sodium distribution from the surface until 6 cm below; right: potassium distribution from the surface until 6 cm below; comparison of quantification via LA-ICP-MS and wet chemistry / AAS analysis

For a qualitative comparison of the alkali profiles in field samples μ -XRF measurements were performed. Figure 3.6 shows the video image and a Na and K map of the same drill core which was analysed by AAS and LA-ICP-MS. For both analytes, no accumulation due to alkali exposure is noted. Differences are due to cement and aggregate type of the upper and the lower course. Sensitivity of the μ -XRF measurement does not seem sufficient to illustrate accumulation of Na in the outer drill core region as differences in concentration might be too small (0.3 – 0.55 m% from 0 – 1 cm and ~0.25 m% > 2 cm in Figure 3.6).

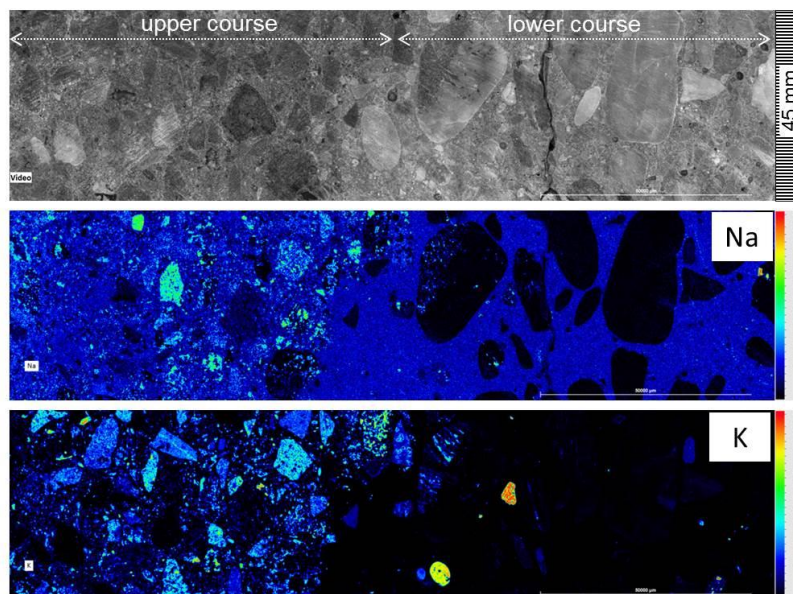


Figure 3.6: μ -XRF mapping of a drill core from a ten year old road construction; concrete surface is on the left; the scala for the intensity of the element signal is on the right; (scan area 45 mm x 181 mm) with a resolution of 75 μ m per pixel with X-ray acquisition using a M4 Tornado plus with Rh tube set to 50 kV at 600 μ A

To constitute the enrichment of alkalis on a laboratory sample (cross section of a 10x10x36 cm prism) the total amount of Na_2O and K_2O was analysed by AAS after one year storage in 4 percent NaOH (Figure 3.7). Similar to the field side, the laboratory sample illustrated in Figure 3.7 shows a significant enrichment of Na on the surface area of the sample. The enrichment factor of Na_2O of the laboratory sample is 4.3 which explains higher reaction affinities. Also the laboratory sample shows slightly fluctuating potassium concentrations in the range of 0.15 to 0.35 m% and no accumulation within the cement stone.

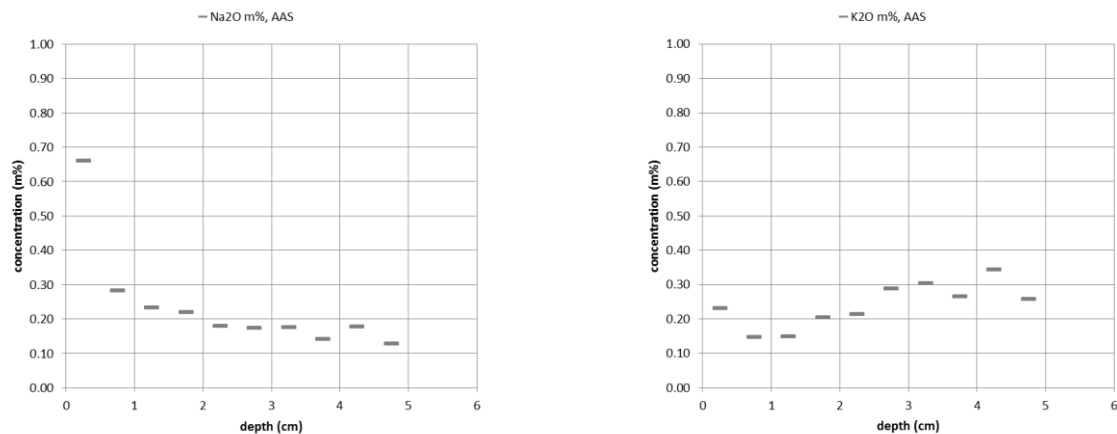


Figure 3.7: concentration of Na_2O and K_2O of a laboratory sample after one year storage in 4 percent NaOH; surface of the sample is on the left

For a qualitative comparison of the alkali profiles in the laboratory sample μ -XRF measurements were performed as well. Figure 3.8 shows the video image and a Na map of the laboratory sample used for the AAS analyses illustrated above. The enrichment of sodium takes place in the first 2 cm below the concrete surface and is twice the factor than in the field sample. Therefore the qualitative difference in the sodium concentration can be illustrated by μ -XRF, using the same analytical setting.

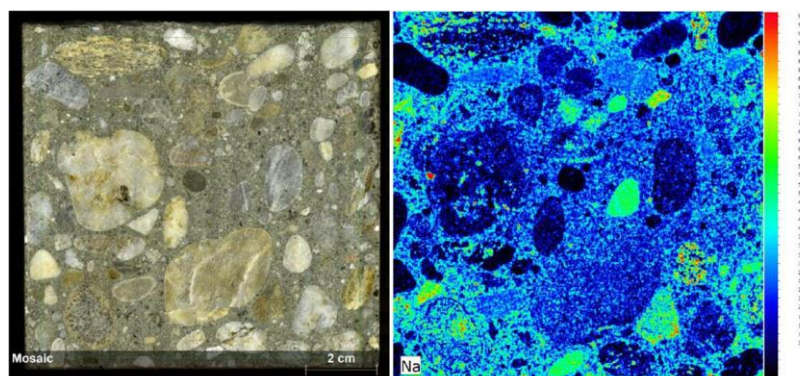


Figure 3.8: left: cross section of a laboratory sample (cross section; prism 10 x 10 x 36 cm) after one year storage in 4 percent NaOH, all sides are concrete surface; the scala for the intensity of the element signal is on the right

4. CONCLUSIONS

First intermediate results of the Austrian research project "AKR – Performance" provide relevant insights into the reliability of national ASR testing. Following statements can be assumed from the current point of view:

- Aggregates with negative test results according to the National Standard  NORM B 3100 do not necessary lead to damages in road constructions.

- The total amount of alkalis (Na_{equ}) and the ratio of Na_{equ} with available quartz in the aggregates show insufficient correlation with the total expansion of ASR laboratory testing. Fluvioglacial gravel (Q1, Q2 and Q3) and paragneiss (Q4) fit in this concept, but metamorphic overprinted aggregates with basaltic chemistry do not.
- Concrete microstructures of field samples show less ASR-products and cracking than laboratory samples after one year storage in 4 percent NaOH.
- LA-ICP-MS and AAS are proper techniques to quantify the total amount of alkalis in concrete samples and the results fit together.
- Both, field and laboratory samples show accumulation of Na_2O up to 2 cm below the concrete surface.
- Potassium shows a similar distribution of concentration within field and laboratory samples.
- μ -XRF mapping of concrete samples with a total amount of < 1 m% alkalis gives good images if the concentration shows differences ≥ 4 . Differences < 4 cannot be visualized by element maps within this concentration range.
- The enrichment of Na_2O of laboratory samples is twice than that of ten year old field samples from road constructions.

5. OUTLOOK

Long-term standard testing will be conducted to evaluate and quantify:

- Influences of cement type,
- total amount of cement,
- alkalinity of the testing solution and
- temperature.

Structural parameters and the formation of ASR-products of tested prisms will be observed by microscopical analyses coupled with image evaluation to determine the volume of ASR-products. Basics for prospective testing in Austria by using a performance approach will be discussed.

6. ACKNOWLEDGEMENTS

The authors gratefully acknowledge the financial support of this project through the Austrian Research Promotion Agency (FFG). Further we thank Dr. Andreas Limbeck from the Institute of Chemical Technologies and Analytics (TU Wien) for facilitating the LA-ICP-MS instrumentation and measurement method. Furthermore we thank Bruker Nano GmbH for providing micro-RFA test measurements.

7. REFERENCES

- [1] Bérubé A, Fournier B, Durand B (2000) Alkali-aggregate reaction in concrete. Proceedings of the 11th International Conference on Alkali-Aggregate Reaction in Concrete, Centre de Recherche Interuniversitaire sur le Béton (CRIB), Québec, Canada
- [2] Tang M, Deng M (2004) Alkali-aggregate reaction in concrete. Proceedings of the 12th International Conference on Alkali-Aggregate Reaction in Concrete, International Academic Publishers, World Publishing Company, Beijing, China
- [3] Dähn R, Arakcheeva A, Schaub P, Pattison P, Chapuis G, Grolimund D, Wieland E, Leemann A (2016) Application of micro X-ray diffraction to investigate the reaction products formed by the alkali-silica reaction in concrete structures. *Cement Concrete Res* 79: 49-56. <https://doi.org/10.1016/j.cemconres.2015.07.012>
- [4] Freyburg E, Schliffkowitz D (2006) Bewertung der Alkalireaktivität von Gesteinskörnungen nach petrographischen und mikrostrukturellen Kriterien. In: 16. ibausil Weimar 2006, Tagungsband 2, S. 355-372

- [5] Gibson C (2013) Dissertation, Die Alkali-Kieselsäure-Reaktion in Beton für Fahrbahndecken und Flugbetriebsflächen unter Einwirkung alkalihaltiger Enteisungsmittel. Fakultät Bauingenieurwesen der Bauhaus-Universität Weimar
- [6] Stark J, Freyburg E, Seyfarth K, Giebson C, Erfurt D (2007) Bewertung der Alkalireaktivität von Gesteinskörnungen. Beton- und Stahlbetonbau. <https://doi.org/10.1002/best.200700562>
- [7] Seyfarth K (2009) AKR-Performance-Prüfung für Fahrbahndecken aus Beton: Erfahrungen aus Labor und Praxis im Vergleich. In: 17. Internationale Baustofftagung (ibautil), Weimar, 2:255-260
- [8] Lindgård J (2013) Dissertation, Alkali-silica reaction (ASR) - Performance testing. Norwegian University of Science and Technology
- [9] Krispel S (2008) Alkali-Aggregate Reaction (AAR) – Mechanismen, Prüfverfahren und Möglichkeiten zur Vermeidung. BMVIT Straßenforschung 580:5–37
- [10] Shi Z, Lothenbach B (2019) Effect of calcium on synthesis of alkali-silica reaction products. ICC 2019, Prague
- [11] Sofia L, Chappex T, Scrivener K (2019) Impact of storage conditions on expansion due to ASR. ICC 2019, Prague
- [12] Passchier CW, Trouw RAJ (2005) Microtectonics. Springer-Verlag Berlin Heidelberg, Germany
- [15] Sommer H (2006) Alkali-Gesteinskörnung-Reaktion – ein Überblick. Schriftenreihe Straßenforschung Bundesministerium für Verkehr Innovation und Technologie, Wien
- [16] ÖNORM B 3100 (2006) Beurteilung der Alkali-Kieselsäure Reaktivität in Beton. Austrian Standards,
- [17] ÖNORM B 3327-1 (2005) Zemente gemäß ÖNORM EN 197-1 für besondere Verwendungen Teil 1: zusätzliche Anforderungen. Austrian Standards, Vienna
- [18] RILEM Recommended Test Method AAR-2 (2015) Detection of Potential Alkali-Reactivity—Accelerated Mortar-Bar Test Method for Aggregates. IN: RILEM State Art Reports, volume 17
- [19] EN 13657 (2002) Charakterisierung von Abfällen – Aufschluss zur anschließenden Bestimmung des in Königswasser löslichen Anteils an Elementen in Abfällen. European Standard, Brussels
- [20] ÖNORM EN 196-2 (2013) Prüfverfahren für Zement – Teil 2: Chemische Analyse von Zement. Austrian Standards, Vienna
- [21] Bonta M, Eitzenberger A, Burtscher S, Limbeck A (2016) Quantification of chloride in concrete samples using LA-ICP-MS. Cement Concrete Res 86:78-84. <http://dx.doi.org/10.1016/j.cemconres.2016.05.002>